

The Z3RO Family of Precoders Cancelling Nonlinear Power Amplification Distortion in Large Array Systems

François Rottenberg, Gilles Callebaut, Liesbet Van der Perre

Abstract—Large array systems use a massive number of antenna elements and clever precoder designs to achieve an array gain at the user location. These precoders require linear front-ends, and more specifically linear power amplifiers (PAs), to avoid distortion. This reduces the energy efficiency since PAs are most efficient close to saturation, where they generate most nonlinear distortion. Moreover, the use of conventional precoders can induce a coherent combining of distortion at the user locations, degrading the signal quality. In this work, novel linear precoders, simple to compute and to implement, are proposed that allow working close to saturation, while cancelling the third-order nonlinearity of the PA without prior knowledge of the signal statistics and PA model. Their design consists in saturating a single or a few antennas on purpose together with an negative gain with respect to all other antennas to compensate for the overall nonlinear distortion at the user location. The performance gains of the designs are significant for PAs working close to saturation, as compared to maximum ratio transmission (MRT) precoding and perfect per-antenna digital pre-distortion (DPD) compensation.

I. INTRODUCTION

A. Problem Statement

Energy efficiency improvements and carbon footprint reduction are main concerns in our society and priorities of governments, such as expressed in Europe’s Green Deal [1]. Inefficient operation of the power amplifier (PA) has been identified as the main contributor to overall energy budget of wireless networks. Indeed, typical spectral efficient transmission schemes exhibit a high dynamic range, calling for a significant back-off in the amplifier operation. This brings about an inevitable trade-off between linearity and efficiency [2]. On the one hand, the linearity of the PA directly impacts the signal quality. On the other hand, the PA has a maximal efficiency when it is operating is close to saturation, where its characteristic is nonlinear and creates distortion. The latter can degrade the quality of the communication link, and moreover generates out-of-band (OOB) distortions. This results in trade-offs between system capacity and power consumption.

Recent works have studied how the transmission with large antenna arrays can impact the trade-off between linearity and energy efficiency [3]–[6]. In massive multiple input multiple output (MIMO) systems, authors have shown that the PA nonlinear distortion is not always uniformly radiated [7], [8]. Measurements performed with an actual massive MIMO testbed also confirmed that the distortion terms can appear as correlated noise and hence can coherently combine [9]. In many situations, nonlinear distortion coherently combines in

the direction(s) of the intended user(s) and more specifically at its location. This is in particular pronounced for a scenario with a single or a few users and dominant propagation direction(s), *e.g.*, a strong line-of-sight (LOS) component. The analysis has been extended to deployments with distributed arrays [10]. When many intermodulation beams [11] appear, with increasing number of users and multi-path components in the channels, the transmit signals become ‘isotropically’ radiated [8]. More importantly, novel precoders designed with adequate performance criteria, as introduced in this paper, can avoid this coherent combining altogether.

B. State-of-the-Art

Allowing the PAs to work close to saturation while preventing degradation of the link quality has been a vast area of research in the literature. One solution is to use a low peak-to-average power ratio (PAPR) waveform or precoding technique, such as the constant-envelope precoder [12]. However, their adoption has been hindered by the associated high digital processing complexity. Another technique is to use reserved tones of an orthogonal frequency division multiplexing (OFDM) system to design a peak-cancelling signal that lowers the PAPR of the signal fed to the PAs [13]. Related challenges are the loss of spectral efficiency and the complexity of optimizing the data-dependent cancelling signal. Another solution is to use digital pre-distortion compensation techniques: the signal that is at the input of the PA is pre-distorted so as to compensate for distortions created by the PA. This enables higher PA efficiencies [14]. It has also been studied for massive MIMO [15], [16]. These techniques are however data-dependent and often require a feedback loop. Applying these techniques requires a certain complexity burden and causes scalability problems, especially in a massive MIMO setting, where it has to be implemented for each PA. Moreover, even a perfect digital pre-distortion only linearizes input signals with an amplitude lower than the saturation level of the PA (weakly nonlinear effects). Higher fluctuations are clipped due to saturation, resulting in nonlinear distortion (strongly nonlinear effects). This phenomenon becomes more likely as the back-off power is reduced, especially for high PAPR signals such as multicarrier and massive MIMO systems. A neural network approach for digital pre-distortion (DPD) has been considered in [17], where the DPD is applied before the precoder and scales with the number of users rather than the number of antennas. Another suggested solution is to use or create differences between the PA characteristics to induce noncoherent combining of distortion at the user location [18].

In contrast to previous techniques, this work focuses on the design of novel linear precoders, which are simple to

François Rottenberg, Gilles Callebaut and Liesbet Van der Perre are with ESAT-DRAMCO, Ghent Technology Campus, KU Leuven, 9000 Ghent, Belgium (e-mail: francois.rottenberg@kuleuven.be).

implement and to compute. A recent work [19] has followed a similar approach. However, no simple closed-form solution for the precoder could be found. An optimization approach is used as the algorithm is iterative, requires computing gradients of large matrices and projections. Moreover, due to the non-concavity of the problem, the authors need to perform the optimization several times with different initialization points. Another recent work [20] has considered the design of linear precoders to null nonlinear distortion towards victim users. The authors used a sub-optimal approach based on constant envelope precoding coefficients. In the work [21], the symbols prior to the PAs are optimized with an iterative algorithm to minimize the mean squared error at the receive side. An iterative algorithm based on zero forcing precoding was considered in [22] to cancel nonlinear distortion and avoid user interference in an OFDM system. The algorithm can also keep out-of-band radiation low so as to preserve spectral purity. As opposed to these previous works, the approach in this work is purely analytical. No iterative algorithms are required and we propose precoders in closed-form. Moreover, no constraint on the envelope of the precoder is imposed, leading to a more performant design.

C. Contributions

In this paper, we present an original contribution: the zero third-order distortion (Z3RO) family of linear precoders which have a low complexity and maximize the received signal-to-noise ratio (SNR) while completely canceling the third-order nonlinear distortion at the user location. More specifically, the structure of our paper and our contributions are structured as follows. Section II describes the system model. Sections III presents the limitation of the maximum ratio transmission (MRT) precoder, *i.e.*, MRT is only optimal in the linear regime. As the PAs enter saturation, MRT is not optimal due to nonlinear distortion. Section IV presents the Z3RO family of linear precoders. We formulate an optimization problem to design the linear precoder that maximizes the SNR at the receiver while completely cancelling the third-order distortion at the user location. The problem is not concave. Still, we solve it and fully characterize its maxima. Each maximum requires to perform a line search. In the pure LOS case, it is shown that all maxima are globally optimal and have a simple closed-form solution. For the general channel case, the so-called Z3RO precoder is proposed based on a heuristic design, which has a simple closed-form and is shown to provide good performance. The Z3RO precoder was initially proposed in [23]. A measurement-based performance evaluation was performed in [24]. The basic principle of the proposed precoders is to use a set of saturated¹ antennas with a negative gain as compared to all other antennas so as to compensate their overall distortion. It is shown that the resulting array gain penalty becomes negligible in the large antenna case, and especially in the saturation regime, where the signal-to-noise-and-distortion ratio (SNDR) is limited by the signal-to-distortion ratio (SDR) and not by the SNR. It is also shown that

¹By “saturated antennas”, we refer to antennas with a relatively higher absolute channel gain than the remaining antennas.

while using a single saturated antenna is optimal in terms of SNR, using more induces a more spatially focused distortion pattern, which is useful regarding unintended locations and OOB radiation. Section V presents simulation results. Finally, Section VI concludes the paper.

Notations: Vectors and matrices are denoted by bold lowercase \mathbf{a} and uppercase letters \mathbf{A} , respectively (*resp.*). Superscripts $*$ and T stand for conjugate and transpose operators. The symbol \mathbb{E} denotes the expectation. j is the imaginary unit. \mathbf{I}_N denotes the identity matrix of order N . The notation $\text{diag}(\mathbf{a})$ refers to a diagonal matrix whose k -th diagonal entry is equal to the k -th entry of vector \mathbf{a} . The notation \mathbf{g}^a element-wise takes the a -th power \mathbf{g} .

II. SYSTEM MODEL

A. Signal Model

We consider a large array-based system with a single user and single base station (BS) equipped with M antennas. The complex symbol intended for the user is denoted by s , with zero mean and variance $p = \mathbb{E}(|s|^2)$. The signal s is precoded at transmit antenna m using a precoder coefficient w_m . The complex baseband representation of the signal before the PA of the corresponding antenna is denoted by x_m and is given by $x_m = w_m s$.

B. Power Amplifier Model

In the following, all PAs are assumed memoryless and have the same transfer function. Their identical nature can be seen as a worst case in terms of coherent combining of distortion [18]. For the sake of clarity and without loss of generality, the linear gain of the PA is set to one. We only consider the third order nonlinear distortion of the PA. This approximation regime is valid as the PA enters saturation regime, which creates nonlinear distortion but not enough for higher order terms to provide a significant contribution. Under these assumptions, the PA output of antenna m can be written as

$$y_m = x_m + a_3 x_m |x_m|^2, \quad (1)$$

where the coefficient a_3 characterizes the nonlinear characteristic of the PA, including both amplitude-to-amplitude modulation (AM/AM) and amplitude-to-phase modulation (AM/PM).

In the simulation section, a more general PA model, not limited to the third order, will be considered for validation purposes.

C. Channel Model

The complex channel gain from antenna m to the user is denoted by h_m . The received signal is given by

$$r = \sum_{m=0}^{M-1} h_m y_m + v, \quad (2)$$

where v is zero mean circularly symmetric complex Gaussian noise with variance σ_v^2 . In the following, at some places, a

pure LOS channel will be considered. In this particular case, h_m can be written as

$$h_m = \sqrt{\beta} e^{-j\phi_m}. \quad (3)$$

The real positive coefficient β models the path loss. The difference of propagation distance between each of the antennas and the user results in an antenna-dependent phase shift ϕ_m , which can be directly related to the antenna location and the angular direction of the user. For a uniform linear array (ULA) and a narrowband system, the phase shift is given by $\phi_m = m \frac{2\pi}{\lambda_c} d \cos(\theta)$, where λ_c is the carrier wavelength, d the inter-antenna spacing and θ is the user angle.

The radiation pattern in an arbitrary direction $\tilde{\theta}$ can be computed as

$$P(\tilde{\theta}) = \mathbb{E} \left(\left| \sum_{m=0}^{M-1} y_m e^{-j\tilde{\phi}_m} \right|^2 \right), \quad (4)$$

where $\tilde{\phi}_m = m \frac{2\pi}{\lambda_c} d \cos(\tilde{\theta})$. Defining the total transmit power $P_T = \int_{-\pi}^{\pi} P(\tilde{\theta}) d\tilde{\theta}$, the array directivity is $D(\tilde{\theta}) = \frac{P(\tilde{\theta})}{P_T/2\pi}$, *i.e.*, $P(\tilde{\theta})$ is normalized with respect to an isotropic radiator. In the following, the radiation and directivity pattern of the linear and nonlinear parts of the amplified signal are depicted in several figures. They are respectively obtained by replacing y_m in (4) by x_m and $a_3 x_m |x_m|^2$.

III. MAXIMUM RATIO TRANSMISSION PRECODER

The well known MRT precoder is obtained by maximizing the received SNR under a transmit power constraint, disregarding the nonlinear distortion terms at the output of the PA. Its expression and the SNR at the user are given by [25]

$$w_m^{\text{MRT}} = \frac{h_m^*}{\sqrt{\sum_{m'=0}^{M-1} |h_{m'}|^2}}, \quad \text{SNR}^{\text{MRT}} = \frac{p \sum_{m'=0}^{M-1} |h_{m'}|^2}{\sigma_v^2}.$$

The MRT achieves an array gain of a factor M . The MRT precoder is optimal as long as the PA works in its linear regime. As p increases, nonlinear terms will be amplified and distortion becomes non-negligible. The PA output y_m given in (1) can be evaluated for $x_m = w_m^{\text{MRT}} s$

$$y_m = s\alpha h_m^* + a_3 s |s|^2 \alpha^3 h_m^* |h_m|^2,$$

where $\alpha = 1/\sqrt{\sum_{m'=0}^{M-1} |h_{m'}|^2}$. The received signal (2) becomes

$$r = s\alpha \sum_{m=0}^{M-1} |h_m|^2 + a_3 s |s|^2 \alpha^3 \sum_{m=0}^{M-1} |h_m|^4 + v.$$

This expression shows that the channel coherently combines both the linear term and the nonlinear term, *i.e.*, their phases are matched. As a result, distortion coherently adds up at the user location and becomes the limiting factor at high power. To illustrate this, let us consider the pure LOS channel introduced in (3). Then,

$$\begin{aligned} y_m &= \frac{e^{j\phi_m}}{\sqrt{M}} (s + a_3 s |s|^2) \\ r &= \sqrt{\beta M} (s + a_3 s |s|^2) + v, \end{aligned}$$

where it is clear that the array gain M affects both linear and nonlinear terms. Moreover, one can see that both the linear and nonlinear terms are beamformed in the same direction, as they are both affected by the term $e^{j\phi_m}$. An example of the directivity pattern of linear/nonlinear terms for a ULA is shown in Fig. 1 (a).

IV. ZERO THIRD-ORDER (Z3RO) FAMILY OF PRECODERS

The MRT precoder induces a coherent combining of distortion at the user location, as demonstrated in the previous section. As p increases, the PAs will become more saturated and the user performance will be limited by its signal-to-distortion ratio (SDR). This section presents the family of Z3RO precoders, which are designed to maximize the SNR at the user location while cancelling the combining of third order distortion.

Inserting (1) in (2), the received signal at the user location for a general linear precoder w_m is

$$r = s \sum_{m=0}^{M-1} h_m w_m + a_3 s |s|^2 \sum_{m=0}^{M-1} h_m w_m |w_m|^2 + v.$$

The distortion term can be forced to zero by ensuring that

$$\sum_{m=0}^{M-1} h_m w_m |w_m|^2 = 0. \quad (5)$$

This constraint does not depend on the transmit symbol s and the PA parameter a_3 , which makes it practical to implement. A similar condition was obtained in [19]. However, the authors made the pessimistic conclusion that considering this constraint leads to a considerable reduction of array gain. Indeed, take the two antenna case $M = 2$ and a LOS channel $h_m = \sqrt{\beta} e^{-j\phi_m}$. If the user angle is coming from broadside, it implies that $\phi_0 = \phi_1 = 0$ and the constraint (5) implies that

$$w_0 |w_0|^2 = -w_1 |w_1|^2 \Leftrightarrow w_0 = -w_1,$$

which leads to a zero array gain, *i.e.*, $|w_0 + w_1|^2 = 0$. The same result occurs for any user angle, as depicted in Fig. 1 (b). However, it is shown further that, with the proposed designs, as the number of antennas M grows large, the loss in array gain becomes negligible, as depicted in Fig. 1 (c) and (d). The precoder optimization problem can be formulated as

$$\max_{w_0, \dots, w_{M-1}} \text{SNR} = \frac{p}{\sigma_v^2} \left| \sum_{m=0}^{M-1} h_m w_m \right|^2, \quad (6)$$

under the two constraints

$$\text{Transmit power: } \sum_{m=0}^{M-1} |w_m|^2 = 1, \quad (7)$$

$$\text{Zero third-order distortion: } \sum_{m=0}^{M-1} h_m w_m |w_m|^2 = 0. \quad (8)$$

Constraint (7) is not exactly a transmit power constraint as the nonlinear transmitted power is disregarded. Given the saturation effect of the PA, it can be seen as an upper bound on the actual transmit power. This choice is made here for simplicity and for the sake of comparison with the MRT

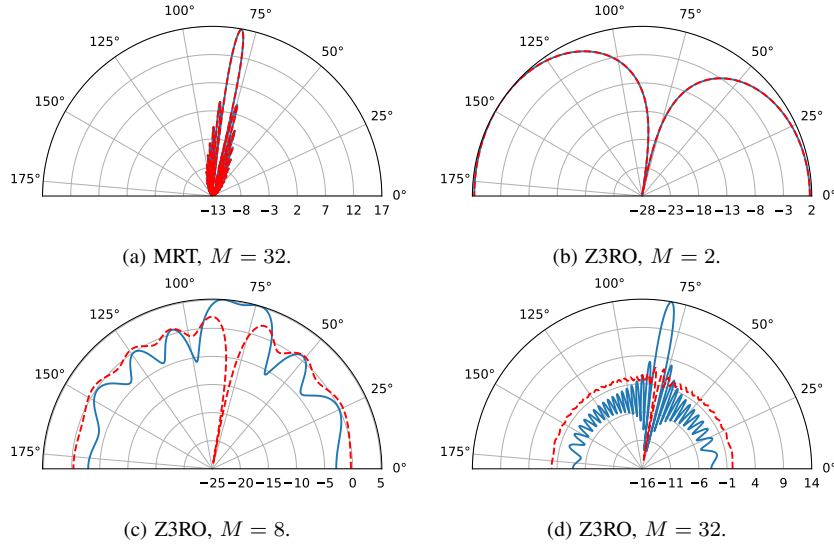


Fig. 1. Directivity pattern [dB] of the signal (continuous blue) and third-order distortion (dashed red) for a pure LOS channel and half-wavelength ULA. User angle is $\theta = 80^\circ$ and $M_s = 1$ saturated antenna. For MRT, distortion coherently combines in the user direction while it is null for Z3RO. The array gain penalty is infinite for $M = 2$ while it vanishes as M grows large.

precoder, which is found under a similar constraint. Moreover, this choice is a good approximation. Even if nonlinearities are considered in this work, we consider a regime where they may have a strong impact on the SDR while having a limited impact on the total transmit power. As a simple example, consider an antenna with 4% nonlinear distortion power with respect to the total transmit power. This might be negligible in terms of transmit power while the SDR is limited to about 14 dB only. It thus makes sense to neglect them in the transmit power computation but consider them in the SNDR expression.

The above problem is non-concave and not trivial to solve. However, it can be first reformulated in a simpler form using the change of variable $w_m = g_m e^{-j\angle h_m}$. Defining $r_m = |h_m|$, the reformulated problem becomes

$$\max_{g_0, \dots, g_{M-1}} \left| \sum_{m=0}^{M-1} r_m g_m \right|^2 \quad \text{s.t.} \quad \sum_{m=0}^{M-1} |g_m|^2 = 1, \quad (9)$$

$$\sum_{m=0}^{M-1} r_m g_m |g_m|^2 = 0.$$

For a given g_m , w_m can be retrieved as $w_m = g_m e^{-j\angle h_m}$. From the above formulation, a conjecture can be made. In the following, to avoid equivalent symmetric solutions, we implicitly constrain the precoders to lead to a real and positive array gain $\sum_{m=0}^{M-1} r_m g_m$. Indeed, one can insert $w_m e^{j\phi}$ with $\phi \in \mathbb{R}$ in (6) and easily check that the array gain is equal to the one achieved by w_m while (7) and (5) still hold. From the formulation (6), a conjecture can be made.

Conjecture 1. An optimal g_m for problem (9) should be purely real up to a constant phasor.

Proof. This conjecture is not yet rigorously proven. Still, clarifying elements are provided in Appendix VII-A. \square

Using this conjecture, the problem is converted to an all

real problem

$$\max_{g_0, \dots, g_{M-1}} \left(\sum_{m=0}^{M-1} r_m g_m \right)^2 \quad \text{s.t.} \quad \sum_{m=0}^{M-1} g_m^2 = 1, \quad \sum_{m=0}^{M-1} r_m g_m^3 = 0, \quad (10)$$

In the following, we always assume that $r_m > 0$, $\forall m$. Otherwise the zero gain antennas can be set inactive and discarded from the optimization. Moreover, we define α in a general sense as a normalization constant that ensures that the transmit power constraint is satisfied, *i.e.*, for a given precoder, real g_m or complex w_m , α is given by

$$\alpha = \frac{1}{\sqrt{\sum_{m=0}^{M-1} g_m^2}} = \frac{1}{\sqrt{\sum_{m=0}^{M-1} |w_m|^2}}. \quad (11)$$

The maxima of (10) are given in the following theorem.

Theorem 1 (Maxima). Problem (10) has M potential maxima. Indexing them by $m' = 0, \dots, M-1$, the m' -th maximum is feasible if there is a positive and real constant ξ which is the solution of the equation

$$\sum_{m=0, m \neq m'}^{M-1} \frac{(-1 + \sqrt{1 + r_m^2 \xi})^3}{r_m^2} = \frac{(1 + \sqrt{1 + r_{m'}^2 \xi})^3}{r_{m'}^2}.$$

The maximum is then obtained by using the precoder

$$g_{m,m'} = \alpha \begin{cases} \frac{-1 + \sqrt{1 + r_m^2 \xi}}{r_m} & \text{if } m \neq m' \\ \frac{-1 - \sqrt{1 + r_m^2 \xi}}{r_m} & \text{if } m = m' \end{cases}.$$

Proof. See Appendix VII-B. \square

Remark 1 (Saturated antenna). Each maximum is obtained by using a single antenna with a negative gain and saturated in such a way that its nonlinear distortion cancels the aggregated nonlinear distortion of all other antennas at the user location. In other words, distortion is used and amplified to cancel distortion. There is a certain analogy possible with the tone

reservation technique [13]. The main difference is that, here, the cancelling elements are in the space domain and not in the frequency domain. Hence, they do not lead to a loss of spectral utilization. They also rely on the saturation of the cancelling elements to be more energy-efficient.

Remark 2 (Global maximum). Finding the global optimum of (10) requires finding the maximum among the M maxima. This is studied via simulations in Section V (Fig. 4). It is shown that the maxima are close to the global one as long as the saturated antenna has a gain r_m close to the median of all r_m . For typical channel gains that we simulated, all maxima were found to be feasible. Non-feasible maxima were found in pathological cases where the channel gain of the saturated antenna $r_{m'}$ is very large, *e.g.*, more than 20 dB above the average of the other ones.

To avoid having to perform the line search procedure and having to search among the different maxima, we present in the following the so-called Z3RO precoder which has a closed-form expression. We also show that, while inducing an array gain penalty, using more than one antenna with negative gains can be useful in practice.

A. Line-of-Sight Channel

Corollary 1 (Z3RO precoder in LOS). For the pure LOS channel given in (3), all maxima of (10) are global maxima, *i.e.*, achieve the same array gain. The m' -th maxima is then given by

$$g_{m,m'} = \alpha \begin{cases} 1 & \text{if } m \neq m' \\ -(M-1)^{1/3} & \text{if } m = m' \end{cases}$$

Moreover, critical points of (10), are obtained by defining a set \mathcal{M} of M_s antennas, chosen arbitrarily among the M antennas with $M/2 > M_s > 0$, and using the precoder

$$g_{m,\mathcal{M}}^{\text{Z3RO}} = \alpha \begin{cases} -\left(\frac{M-M_s}{M_s}\right)^{1/3} & \text{if } m \in \mathcal{M} \\ 1 & \text{otherwise} \end{cases}$$

The SNR at the user is

$$\text{SNR}_{\text{LOS}}^{\text{Z3RO}} = \frac{\beta p}{\sigma_v^2} M \frac{(\zeta^{2/3} - (1-\zeta)^{2/3})^2}{\zeta^{1/3} + (1-\zeta)^{1/3}}, \quad (12)$$

where $\zeta = M_s/M$. For a fixed value of M_s ,

$$\lim_{M \rightarrow +\infty} \frac{\text{SNR}_{\text{LOS}}^{\text{Z3RO}}}{\text{SNR}_{\text{MRT}}} = 1.$$

The array gain penalty versus MRT vanishes.

Proof. See Appendix VII-C. \square

Remark 3 (Saturated antennas). The critical points are obtained by using M_s antennas with a negative gain and saturated in such a way that they compensate for the nonlinear distortion of all other antennas at the user location. Using $M_s = 1$ gives the global optimum.

Remark 4 (Array gain). This precoder is proposed for large array systems, operating in the saturation regime, where SDR

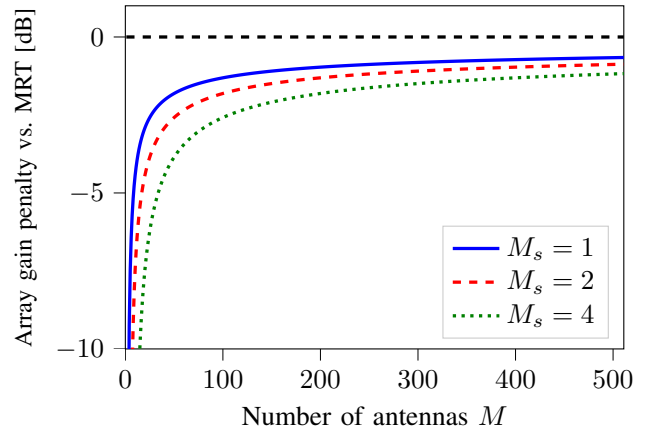


Fig. 2. As the number of antennas increases, the penalty in array gain of the Z3RO precoder vanishes, as compared to MRT. M_s is the number of saturated antennas (with negative gains).

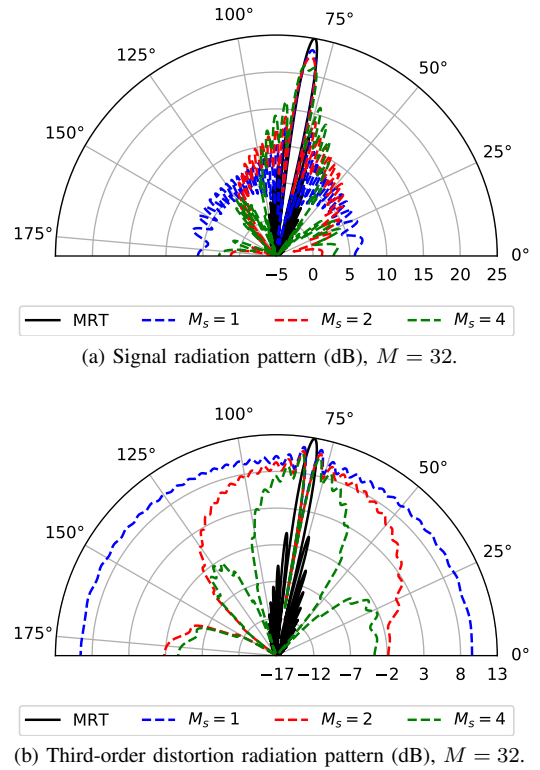


Fig. 3. Radiation pattern for LOS channel and half-wavelength ULA. As more antennas become saturated ($M_s \nearrow$), the array gain of the Z3RO precoder decreases. On the other hand, the total radiated power decreases and it becomes more spatially focused, which is beneficial regarding unintended directions.

is limiting rather than SNR. As a result, the reduced array gain with respect to MRT becomes negligible. Moreover, as shown in Fig. 2, this array gain penalty vanishes for large array systems, as M grows large. For $M_s = 1$ and $M = 64$, the MRT precoder achieves an array gain of about 18 dB versus 16.5 dB for the proposed precoder, while the third distortion order is completely cancelled.

Remark 5 (Radiation pattern). Fig. 1 shows directivity patterns of the signal and distortion for the MRT and the optimal

precoder for $M_s = 1$. On the other hand, Fig. 3 shows their absolute radiation pattern for different values of M_s . In Fig. 3 (a), the array gain decreases when M_s increases. This would imply only using the design $M_s = 1$. However, as shown in Fig. 3 (b), this design, as compared to MRT, leads to an increase of total distortion power, which is mainly radiated towards unintended locations. This leads to interference for potential observers, especially since PA nonlinearities induce out-of-band emissions. Hence, a user in an adjacent band could suffer from it. On the other hand, as M_s increases, the distortion becomes focused “approximately in the user direction, except for the exact user direction, where it is null by design”. Moreover, the total radiated distortion power is reduced. This comes from the fact that distortion is beamformed and benefits from an array gain. As a result, choosing the value M_s offers a trade-off between array gain and spatial focusing of the distortion.

B. General Channel

Inspired by the structure of critical points in the LOS case, we propose a heuristic precoder for the general channel case.

Heuristic 1 (Z3RO precoder). The following heuristic precoder achieves a good performance. Defining a set \mathcal{M} of M_s antennas, chosen arbitrarily among the M antennas with $M/2 > M_s > 0$, choose

$$g_{m,\mathcal{M}}^{\text{Z3RO}} = \alpha r_m \begin{cases} \left(\frac{\sum_{m'=M_s}^{M-1} r_{m'}^4}{\sum_{m''=0}^{M_s-1} r_{m''}^4} \right)^{1/3} & \text{if } m \in \mathcal{M} \\ 1 & \text{otherwise} \end{cases} \quad (13)$$

It will be illustrated through numerical simulations that this precoder yields a negligible array gain penalty as compared to the optimal one. The following remark and proposition give insight on why the heuristic precoder (13) performs well for LOS and general channels respectively.

Proposition 1 (Z3RO performance in LOS). For the pure LOS channel given in (3), the Z3RO precoder (13) reduces to the one of Corollary 1. This explains why the same precoder notation $g_{m,\mathcal{M}}^{\text{Z3RO}}$ has been used. This also implies that, for $M_s = 1$, it is optimal.

Proof. The proof results from a straightforward particularization to the LOS case $r_m = \sqrt{\beta}$. \square

Proposition 2 (Z3RO performance in large antenna systems). If the channel gains r_m are independent and identically distributed (i.i.d.) with variance β , as M and M_s grow large with a fixed ratio $\zeta = M_s/M$,

$$\frac{\text{SNR}_{\text{Z3RO}}}{\text{SNR}_{\text{LOS}}^{\text{Z3RO}}} \rightarrow 1,$$

where SNR_{Z3RO} is the SNR achieved by the heuristic precoder (13) and $\text{SNR}_{\text{LOS}}^{\text{Z3RO}}$ is the one in the deterministic LOS case (12).

Proof. See Appendix VII-D. \square

The previous propositions imply that the performance of the heuristic Z3RO precoder for a general channel and a large

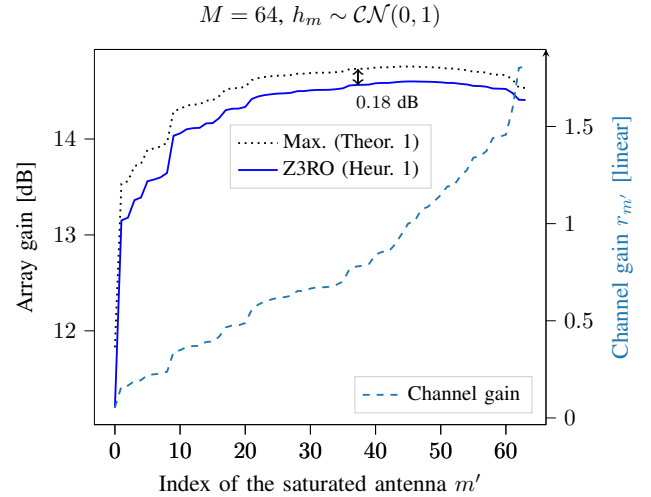


Fig. 4. Array gain as a function of the saturated antenna m' for the maxima described in Theorem 1 and the Z3RO precoder in Heuristic 1 ($\mathcal{M} = \{m'\}$). The right y axis gives the corresponding channel gain $r_{m'} = |h_{m'}|$. Antenna indices are sorted from lowest channel gain to highest.

antenna system are close to the one of the optimal precoder in LOS channel.

V. SIMULATION RESULTS

This section provides a simulation-based validation of the proposed precoders. The MRT is used as a benchmark. Two types of channels are considered. Firstly, the pure LOS channel given in (3) with $\beta = 1$. The phases ϕ_m are set to zero. Another choice would not have affected performance. Secondly, a general channel is used with i.i.d. Rayleigh distributed components. This often considered model does not assume any spatial correlation between antennas. Performance evaluation of the Z3RO precoder based on real-life channel measurements was performed in [24].

A. Comparison of Local and Global Maxima

As explained in Corollary 1, in pure LOS, all maxima of (10) are equally optimal. On the other hand, it is not the case for a general channel. Fig. 4 shows the array gain achieved by the M maxima described in Theorem 1. Indices of antennas are sorted by magnitude of their channel gain, which is also plotted with respect to the right y axis. One can check that the maxima obtained by using the saturated antenna with maximum or minimum channel gain is further from the global maximum. On the other hand, choosing any of the antennas close to the median of the channel gain gives a performance close to the optimal one. In particular, antennas with a relatively low channel gain should be avoided as they require a very high gain to compensate for the distortion of all other antennas. This gives a general and practical guideline to choose which antenna has to be saturated, without having to compare all maxima, as discussed in Remark 2.

B. Comparison of Heuristic Z3RO versus Optimal Precoder

Fig. 4 additionally shows the array gain achieved by the heuristic Z3RO precoder described in Heuristic 1, using the

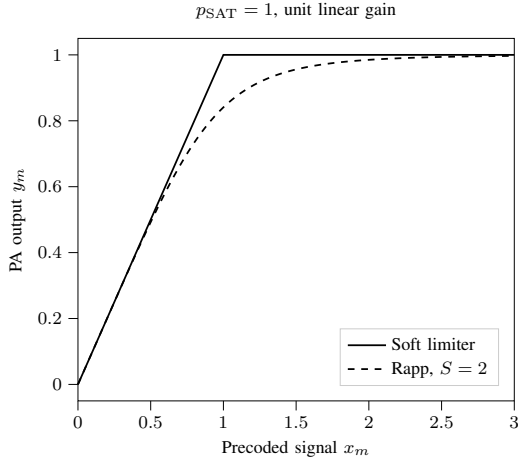


Fig. 5. Two power amplifier models: soft limiter [26] and Rapp [27].
 $M = 64$, $h_m \sim \text{LOS}$, $M_s = 4$, Rapp PA, $\frac{M\beta p}{\sigma_v^2} = 26$ dB

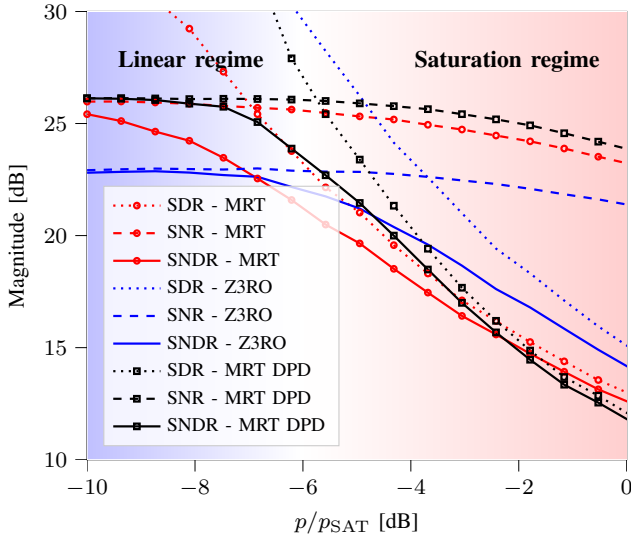


Fig. 6. SNR, SDR and SNDR of the MRT versus Z3RO precoders as a function of the back-off (fixed $p_{\text{PA}} = p/M$, varying p_{SAT}). The Z3RO precoder outperforms MRT in the saturation regime, even with a perfect DPD implemented.

same antenna as the saturated one. The Z3RO precoder achieves a close-to-optimal performance, with a penalty of about 0.18 dB.

C. SNR, SDR and SNDR for Practical PA Models

We now study the performance for two more practical PA models, not limited to a third-order model. They are depicted in Fig. 5. The Rapp PA model [27] is given by

$$y_m = \frac{x_m}{\left(1 + \left|\frac{x_m}{\sqrt{p_{\text{sat}}}}\right|^{2S}\right)^{\frac{1}{2S}}},$$

where S is a smoothness parameter and p_{sat} is the maximal output power of the PA. As $S \rightarrow +\infty$, we obtain the soft limiter model [26]

$$y_m = \begin{cases} x_m & \text{if } x_m \leq \sqrt{p_{\text{sat}}} \\ \sqrt{p_{\text{sat}}} & \text{otherwise} \end{cases},$$

which can be seen as the input of the antenna m provided that perfect per-antenna DPD has been applied before the PA [14]. Note that this induces a significant complexity and the DPD typically only compensates for weakly nonlinear effects while the clipping due to the finite p_{sat} , *i.e.*, the strongly nonlinear effects, is not compensated.

We compare the SNR, SDR and SNDR of the MRT and the Z3RO precoders. The Bussgang theorem [28], [29] implies that the received signal can be decomposed as $r = Gs + d + v$, where d is the nonlinear distortion, which is uncorrelated with the transmit signal s and noise v . The linear gain G can be evaluated as $G = \mathbb{E}(rs^*)/p$. The signal variance is given by $|G|^2 p$. Using the fact that s , v and d are uncorrelated, the distortion variance is $\mathbb{E}(|d|^2) = \mathbb{E}(|r|^2) - |G|^2 p - \sigma_v^2$. The SNR, SDR and SNDR are thus given by

$$\text{SNR} = \frac{|G|^2 p}{\sigma_v^2}, \quad \text{SDR} = \frac{|G|^2 p}{\mathbb{E}(|d|^2)}, \quad \text{SNDR} = \frac{|G|^2 p}{\mathbb{E}(|d|^2) + \sigma_v^2},$$

where the expectations can be evaluated using the statistics of the transmit symbols s .

For a pure LOS channel, Fig. 6 shows the evolution of the SNR, SDR and SNDR of the Z3RO versus MRT precoder as a function of the back-off at each antenna $p_{\text{PA}}/p_{\text{SAT}}$, where $p_{\text{PA}} = p/M$. The simulation parameters are: $S = 2$, $M = 64$, $M_s = 4$, $\frac{M\beta p}{\sigma_v^2} = 26$ dB, the saturation power p_{SAT} is varied while p remains fixed. The soft limiter model is used to evaluate the performance of a perfect DPD. The signal s has a complex Gaussian distribution. For low values of $p_{\text{PA}}/p_{\text{sat}}$, the PA is in the linear regime and the MRT achieves an optimal performance. The Z3RO precoder performs not as well given its reduced array gain. As the ratio $p_{\text{PA}}/p_{\text{sat}}$ increases, the PA enters the saturation regime and distortion becomes non-negligible. MRT is outperformed by the Z3RO precoder, which is only limited by distortion orders higher than three. The perfect DPD implemented with an MRT precoder can only compensate for weakly nonlinear effects and therefore only improves MRT performance when the PA enters saturation. Close to saturation, the strongly nonlinear effects, which are not compensated by the DPD, take over and it is also outperformed by the Z3RO precoder. In conclusion, the advantages of the Z3RO precoder versus MRT (with or without DPD) can be seen in two ways, in the saturation regime:

1) For a same SNDR, the Z3RO precoder can work at a larger ratio $p_{\text{PA}}/p_{\text{sat}}$, implying an enhanced energy efficiency. As an example, to achieve a SNDR of 15 dB the Z3RO precoder can work with a ratio $p_{\text{PA}}/p_{\text{sat}}$, which is about 1.5 dB higher.

2) For a same $p_{\text{PA}}/p_{\text{sat}}$, the Z3RO precoder achieves a larger SNDR, implying an enhanced capacity. As an example, for $p_{\text{PA}}/p_{\text{sat}} = -2$ dB, the SNDR can be boosted by about 2 dB.

Fig. 7 considers the same simulation parameters as Fig. 6. The only difference is that p and thus $p_{\text{PA}} = p/M$ is varied, while the saturation power p_{SAT} remains fixed. As the back-off $p_{\text{PA}}/p_{\text{sat}}$ increases, the SNR of both precoders improves but their SDR degrades. Here again, MRT is only optimal in the linear regime while it is outperformed by the Z3RO precoder in the saturation regime. The DPD improves the SDR

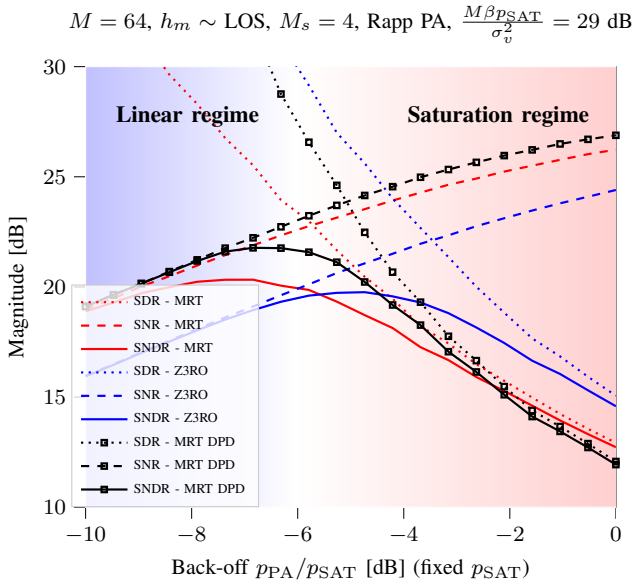


Fig. 7. SNR, SDR and SNDR of the MRT versus Z3RO precoders as a function of the back-off (fixed p_{SAT} , varying p_{PA}). The Z3RO precoder outperforms MRT in the saturation regime, even with a perfect DPD implemented.

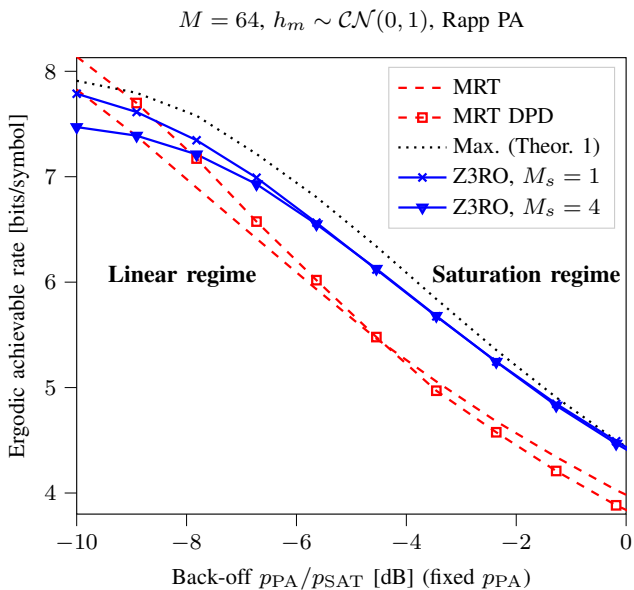


Fig. 8. Ergodic achievable rates of the MRT, maxima of Theorem 1 and Z3RO precoder as a function of the back-off (fixed p_{PA} , varying p_{SAT}).

performance of MRT but this improvement disappears far in the saturation regime due to clipping.

D. Ergodic Achievable Rate

The SNDR, computed through the Bussgang theorem, can be converted to an achievable rate R (and thus a lower bound on the capacity), expressed in bits per symbol, by considering the worst case of having noise and distortion Gaussian distributed

$$R = \log_2(1 + \text{SNDR}).$$

Taking the expectation of R with respect to the channel statistics, an ergodic achievable rate is obtained. It is shown in Fig. 8 for a general channel and for the different studied precoders, as a function of the back-off, fixing p and varying p_{SAT} . As the PA enters saturation, MRT is quickly outperformed by the other precoders. In order, the maximum of Theorem 1 outperforms the Z3RO precoders. The $M_s = 1$ Z3RO precoder performs relatively better than the $M_s = 4$ version due to its higher array gain. Still, further into saturation, except MRT, their performance converges. This can be intuitively explained by the fact that the performance is limited by the SDR and not the SNR, implying that an array gain penalty becomes less detrimental in that regime.

VI. CONCLUSION

In this work, a novel family of linear precoders, the so-called Z3RO family, are proposed for large array-based transmission to allow operating the PAs in an energy efficient operation point closer to saturation. Their implementation has a similar complexity as MRT. In addition, they cancel the third-order distortion at the user location, without requiring knowledge of the PA model and the channel statistics. Their array gain penalty is shown to become negligible for large antenna arrays and especially in the saturation regime. The optimal precoder has no closed-form solution for a general channel. Therefore, the Z3RO precoder was proposed, having a closed-form solution, which is optimal for a pure LOS channel and achieves a good performance for a general channel. Perspectives include the extension to wideband channels, inter-user interference cancellation and PA mismatch. The study of the impact of pilot contamination and channel estimation errors is important in future R&D.

VII. APPENDIX

A. Reasoning behind Conjecture 1

Looking at (9), if the zero third-order distortion constraint vanishes, it is clear that it is better to have all g_m real and positive to maximize the array gain, as MRT does. However, the zero third-order constraint implies that at least one antenna gain should have an opposite polarity, which degrades the array gain through destructive interference. Several choices are possible for the gains of the antennas with opposite polarity, including complex gains. However, to minimize the array gain degradation, given the transmit power constraint, it is intuitively better to use one strongly saturated (high absolute gain) with opposite polarity rather than several ones being less saturated. Due to the third order, the antenna with opposite polarity “might just be slightly more amplified” to compensate for the distortion of all others while consuming a minimal transmit power and degrading only slightly the array gain. If a single antenna is used to compensate for the distortion of all others, its polarity should be opposite and thus negative. The problem then becomes fully real-valued. These considerations were confirmed by extensive simulations based on available solvers, for various channel realizations and using different initialization points given the non-concavity of the objective function.

B. Proof of Theorem 1

1) *Critical Points based on First-Order Conditions:* The Lagrangian formulation of problem (10) is

$$L = \left(\sum_{m=0}^{M-1} g_m r_m \right)^2 - \lambda \left(\sum_{m=0}^{M-1} g_m^2 - 1 \right) - \mu \sum_{m=0}^{M-1} r_m g_m^3.$$

The critical points are obtained by setting the derivatives with respect to g_0, \dots, g_{M-1} to zero while ensuring that the two constraints are satisfied. The derivative with respect to g_m is given by

$$\begin{aligned} \frac{\partial L}{\partial g_m} &= 0 \\ \Leftrightarrow 0 &= -3r_m \mu g_m^2 - 2\lambda g_m + 2r_m \sum_{m'=0}^{M-1} g_{m'} r_{m'}, \end{aligned} \quad (14)$$

whose two possible solutions are given by

$$g_m = \frac{-\lambda \pm \sqrt{\lambda^2 + 6r_m^2 \mu \sum_{m'=0}^{M-1} g_{m'} r_{m'}}}{3\mu r_m}. \quad (15)$$

Now, multiplying (14) by g_m and summing over m gives

$$\begin{aligned} 0 &= -3\mu \sum_{m=0}^{M-1} r_m g_m^3 - 2\lambda \sum_{m=0}^{M-1} g_m^2 + 2 \left(\sum_{m'=0}^{M-1} g_{m'} r_{m'} \right)^2 \\ \lambda &= \left(\sum_{m'=0}^{M-1} g_{m'} r_{m'} \right)^2, \end{aligned} \quad (16)$$

where we used the two constraints in (10), which should be satisfied for a feasible solution. We thus see that λ is given by the squared array gain and is thus positive. As explained before Theorem 1, to avoid symmetric equivalent solution, we constrain the solution to lead to a strictly positive array gain. Hence, we can write

$$\sqrt{\lambda} = \sum_{m'=0}^{M-1} g_{m'} r_{m'} > 0. \quad (17)$$

Inserting this result into (15) gives

$$\begin{aligned} g_m &= -\frac{\lambda}{3\mu r_m} \pm \sqrt{\frac{\lambda^2}{9\mu^2 r_m^2} + \frac{2}{3\mu} \sqrt{\lambda}} \\ &= \alpha \frac{-1 \pm \sqrt{1 + r_m^2 \xi}}{r_m}, \end{aligned} \quad (18)$$

where $\alpha = \frac{\lambda}{3\mu}$ and $\xi = \frac{6\mu}{(\xi\alpha)^2}$. They can be related as $\lambda = \frac{4}{(\xi\alpha)^2}$ and $\mu = \frac{\lambda}{3\alpha} = \frac{4}{(\xi\alpha)^2} \frac{1}{3\alpha}$. From (16), we have $\lambda > 0$. For the third-order nonlinear constraint to be valid, g_m should be allowed to have both positive and negative values that can cancel each other. This implies positiveness of ξ and thus μ and α too. Once the solution \pm for each antenna m is chosen, the values of the constants α and ξ can be found thanks to the two constraints. If the constraints can be satisfied, this results in a given critical point of the problem.

To formalize it, let us define as \mathcal{M}^+ the set of antenna indices where the solution with sign $+$ is chosen, leading to a positive gain g_m . The set of remaining antennas is denoted

by \mathcal{M}^- . These antennas have a negative gain g_m . Then, the zero third-order nonlinear constraint implies that

$$\sum_{m \in \mathcal{M}^+} \frac{(-1 + \sqrt{1 + r_m^2 \xi})^3}{r_m^2} = \sum_{m' \in \mathcal{M}^-} \frac{(1 + \sqrt{1 + r_{m'}^2 \xi})^3}{r_{m'}^2}.$$

The value of ξ is the real positive constant that satisfies this equation. It can be found through, *e.g.*, a line search. This equation does not always have a solution, especially if the cardinality of \mathcal{M}^- is too large and/or the channel gains of antennas in \mathcal{M}^- are large. For a given feasible solution ξ , the value of α corresponds to the normalization constant, which can be found using (11) as

$$\alpha = \frac{1}{\sqrt{\sum_{m \in \mathcal{M}^+} \frac{(-1 + \sqrt{1 + r_m^2 \xi})^2}{r_m^2} + \sum_{m' \in \mathcal{M}^-} \frac{(-1 - \sqrt{1 + r_{m'}^2 \xi})^2}{r_{m'}^2}}}.$$

2) *Maxima based on Second-Order Conditions:* The previous section has given the general structure of the critical points of the problem. We now determine which critical points are maxima by analysing the local concavity of the cost function. More specifically, we first show that i) the critical points characterized by a set \mathcal{M}^- containing more than one antenna cannot be maxima and ii) a set \mathcal{M}^- containing a single element leads to a maximum.

To do this, we study the Hessian of the cost function. We now directly integrate the constraints into the cost function. First of all, the zero third-order nonlinear constraint can be imposed by fixing one of the channel gains. Indeed, without loss of generality, this constraint implies that

$$r_0 g_0^3 = - \sum_{m=1}^{M-1} r_m g_m^3 \Leftrightarrow g_0 = - \left(\sum_{m=1}^{M-1} \frac{r_m}{r_0} g_m^3 \right)^{1/3}.$$

Hence, the optimization can be performed over the remaining variables g_1, \dots, g_{M-1} , while g_0 is fixed by the other ones. Similarly, the transmit power constraint can be imposed on the cost function by using the change of variables

$$g_m = \frac{\tilde{g}_m}{\sqrt{\sum_{m'=0}^{M-1} \tilde{g}_{m'}^2}}, \quad (19)$$

and performing the optimization with respect to \tilde{g}_m . The optimal g_m is then found by normalizing \tilde{g}_m through (19). Hence, problem (10), can be reformulated as

$$\max_{\tilde{g}_1, \dots, \tilde{g}_{M-1}} f(\tilde{g}_1, \dots, \tilde{g}_{M-1}) = \frac{n(\tilde{g}_1, \dots, \tilde{g}_{M-1})}{d(\tilde{g}_1, \dots, \tilde{g}_{M-1})}, \quad (20)$$

where

$$\begin{aligned} n(\tilde{g}_1, \dots, \tilde{g}_{M-1}) &= \left(\sum_{m=1}^{M-1} r_m \tilde{g}_m + r_0 \tilde{g}_0 \right)^2 \\ d(\tilde{g}_1, \dots, \tilde{g}_{M-1}) &= \sum_{m''=1}^{M-1} \tilde{g}_{m''}^2 + \tilde{g}_0^2 \\ \tilde{g}_0 &= - \left(\sum_{m=1}^{M-1} \frac{r_m}{r_0} \tilde{g}_m^3 \right)^{1/3}. \end{aligned}$$

The critical points of (10) are properly normalized so that $g_m = \tilde{g}_m$ and are also critical points of (20). The other way

around, critical points of (20) with a proper normalization (19) are also critical points of (10). Hence, we can study the Hessian of $f(\tilde{g}_1, \dots, \tilde{g}_{M-1})$ at each critical point to determine if the critical points found in (18) are maxima or not.

a) *Hessian Computation:* At the critical points, some simplifications occurs. The (\tilde{m}, \tilde{m}) element of the Hessian matrix is given by

$$\begin{aligned} \frac{\partial^2 f}{\partial \tilde{g}_m \partial \tilde{g}_m} &= \frac{\frac{\partial}{\partial \tilde{g}_m} (\frac{\partial n}{\partial \tilde{g}_m} d - n \frac{\partial d}{\partial \tilde{g}_m}) d^2 - (\frac{\partial n}{\partial \tilde{g}_m} d - n \frac{\partial d}{\partial \tilde{g}_m}) \frac{\partial}{\partial \tilde{g}_m} d^2}{d^4} \\ &= \frac{\partial^2 n}{\partial \tilde{g}_m \partial \tilde{g}_m} - \lambda \frac{\partial^2 d}{\partial \tilde{g}_m \partial \tilde{g}_m}, \end{aligned}$$

where we use the fact that, at critical points, the first order derivative is null, and thus $\frac{\partial n}{\partial \tilde{g}_m} d - n \frac{\partial d}{\partial \tilde{g}_m} = 0$. Moreover, at the critical points (18), $d = 1$ and $n = \lambda$. After several derivations, defining $\mathbf{I} = \mathbf{I}_{M-1}$, $\tilde{\mathbf{g}} = (\tilde{g}_1, \dots, \tilde{g}_{M-1})^T$ and $\mathbf{r} = (r_0, \dots, r_{M-1})^T$, we find

$$\begin{aligned} \mathbf{H} &= \frac{\partial^2 n}{\partial \tilde{\mathbf{g}} \partial \tilde{\mathbf{g}}^T} - \lambda \frac{\partial^2 d}{\partial \tilde{\mathbf{g}} \partial \tilde{\mathbf{g}}^T} \\ &= 2 \left(\mathbf{r} - \frac{1}{\tilde{g}_0^2} \text{diag}(\mathbf{r}) \tilde{\mathbf{g}}^2 \right) \left(\mathbf{r} - \frac{1}{\tilde{g}_0^2} \text{diag}(\mathbf{r}) \tilde{\mathbf{g}}^2 \right)^T \\ &\quad - 2\lambda \left(\mathbf{I} - \frac{2 \text{diag}(\mathbf{r}) \text{diag}(\tilde{\mathbf{g}})}{r_0 \tilde{g}_0} - \frac{\text{diag}(\mathbf{r}) \tilde{\mathbf{g}}^2 (\tilde{\mathbf{g}}^2)^T \text{diag}(\mathbf{r})}{r_0^2 \tilde{g}_0^4} \right) \\ &\quad - 4\sqrt{\lambda} \left(\frac{1}{\tilde{g}_0^3} \text{diag}(\mathbf{r}) \text{diag}(\tilde{\mathbf{g}}) + \frac{\text{diag}(\mathbf{r}) \tilde{\mathbf{g}}^2 (\tilde{\mathbf{g}}^2)^T \text{diag}(\mathbf{r})}{r_0 \tilde{g}_0^5} \right). \end{aligned}$$

At a critical point, we have $\frac{\partial n}{\partial \tilde{\mathbf{g}}} d = n \frac{\partial d}{\partial \tilde{\mathbf{g}}}$. Computing these derivatives, using $d = 1$ and $n = \lambda$, results in

$$\left(\mathbf{r} - \frac{1}{\tilde{g}_0^2} \text{diag}(\mathbf{r}) \tilde{\mathbf{g}}^2 \right) = \sqrt{\lambda} \left(\tilde{\mathbf{g}} - \frac{1}{r_0 \tilde{g}_0} \text{diag}(\mathbf{r}) \tilde{\mathbf{g}}^2 \right).$$

Using this, the Hessian becomes

$$\begin{aligned} \mathbf{H} &= 2\lambda \left(\tilde{\mathbf{g}} - \frac{1}{r_0 \tilde{g}_0} \text{diag}(\mathbf{r}) \tilde{\mathbf{g}}^2 \right) \left(\tilde{\mathbf{g}} - \frac{1}{r_0 \tilde{g}_0} \text{diag}(\mathbf{r}) \tilde{\mathbf{g}}^2 \right)^T \\ &\quad - 2\lambda \left(\mathbf{I} - \frac{2 \text{diag}(\mathbf{r}) \text{diag}(\tilde{\mathbf{g}})}{r_0 \tilde{g}_0} - \frac{\text{diag}(\mathbf{r}) \tilde{\mathbf{g}}^2 (\tilde{\mathbf{g}}^2)^T \text{diag}(\mathbf{r})}{r_0^2 \tilde{g}_0^4} \right) \\ &\quad - 4\sqrt{\lambda} \left(\frac{1}{\tilde{g}_0^2} \text{diag}(\mathbf{r}) \text{diag}(\tilde{\mathbf{g}}) + \frac{\text{diag}(\mathbf{r}) \tilde{\mathbf{g}}^2 (\tilde{\mathbf{g}}^2)^T \text{diag}(\mathbf{r})}{r_0 \tilde{g}_0^5} \right). \end{aligned}$$

b) *Non-Maxima among Critical Points:* We now show that the critical points characterized by a set \mathcal{M}^- containing more than one antenna cannot be maxima. To demonstrate this, we show that the Hessian \mathbf{H} evaluated at these critical points is not negative semi-definite, which implies that the cost function is not locally concave. Thus, no maximum can be found. Let us consider one such critical point with at least two antenna indices belonging to \mathcal{M}^- . With a potential reindexing, we can define two of these indices in \mathcal{M}^- as antennas $m = 0$ and $m = 1$ and we further index them so that $r_1 \geq r_0$. From (18), we can find that $g_0 < 0$ and $g_1 < 0$ and thus, similarly $\tilde{g}_0 = g_0 < 0$ and $\tilde{g}_1 = g_1 < 0$.

A condition for \mathbf{H} to be negative semi-definite is that all of its diagonal elements are negative. Let us focus on its first diagonal element

$$\begin{aligned} [\mathbf{H}]_{0,0} &= 2\lambda \left(\tilde{g}_1 - \frac{r_1 \tilde{g}_1^2}{r_0 \tilde{g}_0} \right)^2 - 2\lambda \left(1 - \frac{2r_1 \tilde{g}_1}{r_0 \tilde{g}_0} - \frac{r_1^2 \tilde{g}_1^4}{r_0^2 \tilde{g}_0^4} \right) \\ &\quad - 4\sqrt{\lambda} \frac{1}{\tilde{g}_0^5} (\tilde{g}_0^3 r_1 \tilde{g}_1 + \frac{r_1^2 \tilde{g}_1^4}{r_0}), \end{aligned}$$

which is the sum of three terms. The first one is clearly positive due to the square and since $\lambda > 0$. The third also, given that $\tilde{g}_0 < 0$, $\tilde{g}_1 < 0$, $r_0 > 0$ and $r_1 > 0$. The second term requires more development. It can be rewritten as

$$2\lambda \left(-1 + \frac{r_1 \tilde{g}_1}{r_0 \tilde{g}_0} (2 + \frac{r_1 \tilde{g}_1^3}{r_0 \tilde{g}_0^3}) \right) \geq 2\lambda \left(-1 + 2 \frac{r_1 \tilde{g}_1}{r_0 \tilde{g}_0} \right).$$

Using (18) and the fact that $r_1 \geq r_0$, we find

$$\frac{r_1 \tilde{g}_1}{r_0 \tilde{g}_0} = \frac{1 + \sqrt{1 + r_1^2 \xi}}{1 + \sqrt{1 + r_0^2 \xi}} \geq 1,$$

and thus

$$2\lambda \left(-1 + \frac{r_1 \tilde{g}_1}{r_0 \tilde{g}_0} (2 + \frac{r_1 \tilde{g}_1^3}{r_0 \tilde{g}_0^3}) \right) \geq 2\lambda > 0.$$

This implies that $[\mathbf{H}]_{0,0} > 0$ and thus, no critical points with negative gains at more than one antenna can lead to a maximum.

c) *Maxima among Critical Points:* We now show that a set \mathcal{M}^- containing a single element leads to a maximum. Let us rearrange antenna indices such that the element in \mathcal{M}^- corresponds to index $m = 0$. From (18), we can find that $g_0 = \tilde{g}_0 < 0$ and $g_m = \tilde{g}_m > 0$, $\forall m \neq 0$. We now need to show that the Hessian \mathbf{H} is semi-definite negative at this critical points. To do this, we use the fact that the sum of negative semi-definite matrices is negative semi-definite. Matrix \mathbf{H} is the sum of matrices multiplied by either λ or $\sqrt{\lambda}$. The group proportional to $4\sqrt{\lambda}$ is

$$-\frac{1}{\tilde{g}_0^2} \text{diag}(\mathbf{r}) \text{diag}(\tilde{\mathbf{g}}) - \frac{1}{r_0 \tilde{g}_0^5} \text{diag}(\mathbf{r}) \tilde{\mathbf{g}}^2 (\tilde{\mathbf{g}}^2)^T \text{diag}(\mathbf{r}).$$

Multiplying this matrix by $\text{diag}(\mathbf{r}^{-1/2}) \text{diag}(\tilde{\mathbf{g}}^{-1/2})$ on the left, on the right and by the scalar \tilde{g}_0^2 does not change its definiteness given that all quantities are positive definite.

$$-\mathbf{I} + \frac{1}{r_0 \tilde{g}_0^3} \text{diag}(\mathbf{r})^{1/2} \tilde{\mathbf{g}}^{3/2} (\tilde{\mathbf{g}}^{3/2})^T \text{diag}(\mathbf{r})^{1/2}.$$

This matrix has all eigenvalues equal to -1 except a single one equal to $-1 - \frac{\mathbf{r}^T \tilde{\mathbf{g}}^3}{r_0 \tilde{g}_0^3} = -1 - \frac{-r_0 \tilde{g}_0^3}{r_0 \tilde{g}_0^3} = 0$. Hence, it is well negative semi-definite. The group proportional to 2λ is

$$\begin{aligned} &\left(\tilde{\mathbf{g}} - \frac{1}{r_0 \tilde{g}_0} \text{diag}(\mathbf{r}) \tilde{\mathbf{g}}^2 \right) \left(\tilde{\mathbf{g}} - \frac{1}{r_0 \tilde{g}_0} \text{diag}(\mathbf{r}) \tilde{\mathbf{g}}^2 \right)^T \\ &\quad - \left(\mathbf{I} - \frac{1}{r_0 \tilde{g}_0} \text{diag}(\mathbf{r}) \text{diag}(\tilde{\mathbf{g}}) \right) \\ &\quad + \frac{1}{r_0 \tilde{g}_0} \text{diag}(\mathbf{r}) \text{diag}(\tilde{\mathbf{g}}) + \frac{1}{r_0^2 \tilde{g}_0^4} \text{diag}(\mathbf{r}) \tilde{\mathbf{g}}^2 (\tilde{\mathbf{g}}^2)^T \text{diag}(\mathbf{r}). \end{aligned}$$

$$\begin{aligned} & \left(\mathbf{I} - \frac{\text{diag}(\mathbf{r})\text{diag}(\tilde{\mathbf{g}})}{r_0\tilde{g}_0} \right)^{1/2} \left[-\mathbf{I} + \left(\mathbf{I} - \frac{\text{diag}(\mathbf{r})\text{diag}(\tilde{\mathbf{g}})}{r_0\tilde{g}_0} \right)^{1/2} \tilde{\mathbf{g}}\tilde{\mathbf{g}}^T \left(\mathbf{I} - \frac{\text{diag}(\mathbf{r})\text{diag}(\tilde{\mathbf{g}})}{r_0\tilde{g}_0} \right)^{1/2} \right] \left(\mathbf{I} - \frac{\text{diag}(\mathbf{r})\text{diag}(\tilde{\mathbf{g}})}{r_0\tilde{g}_0} \right)^{1/2} \\ & + \frac{1}{r_0\tilde{g}_0} \text{diag}(\mathbf{r})\text{diag}(\tilde{\mathbf{g}}) + \frac{1}{r_0\tilde{g}_0^3} \text{diag}(\mathbf{r})\tilde{\mathbf{g}}^2(\tilde{\mathbf{g}}^2)^T \text{diag}(\mathbf{r}). \end{aligned} \quad (21)$$

This can be rewritten as (21). Multiplying (21) by $\text{diag}(\mathbf{r}^{-1/2})\text{diag}(\tilde{\mathbf{g}}^{-1/2})$ on the left and on the right, we get

$$\begin{aligned} & \left(\mathbf{I} - \frac{\text{diag}(\mathbf{r})\text{diag}(\tilde{\mathbf{g}})}{r_0\tilde{g}_0} \right)^{1/2} \tilde{\mathbf{g}}\tilde{\mathbf{g}}^T \left(\mathbf{I} - \frac{\text{diag}(\mathbf{r})\text{diag}(\tilde{\mathbf{g}})}{r_0\tilde{g}_0} \right)^{1/2} \\ & - \mathbf{I} + \frac{1}{r_0\tilde{g}_0} \left(\mathbf{I} + \frac{1}{r_0\tilde{g}_0^3} \text{diag}(\mathbf{r}^{1/2})\tilde{\mathbf{g}}^{3/2}(\tilde{\mathbf{g}}^{3/2})^T \text{diag}(\mathbf{r}^{1/2}) \right). \end{aligned}$$

We can subdivide this matrix in two groups. The first two additive terms give a matrix with all eigenvalues equal to -1 except a single one equal to

$$-1 + \|\tilde{\mathbf{g}}\|^2 - \frac{\mathbf{r}^T \tilde{\mathbf{g}}^3}{r_0\tilde{g}_0} = -1 + 1 - \tilde{g}_0^2 - \frac{-r_0\tilde{g}_0^3}{r_0\tilde{g}_0} = 0.$$

The second group can be multiplied by the positive quantity $-r_0\tilde{g}_0$ without changing the definiteness. The remaining matrix has all eigenvalues equal to -1 except one equal to $-1 - \frac{\mathbf{r}^T \tilde{\mathbf{g}}^3}{r_0\tilde{g}_0^3} = 0$. As a result the group proportional to 2λ is well negative semi-definite and so is the Hessian \mathbf{H} for critical points characterized by a single antenna with negative gain. This concludes the proof of Theorem 1.

C. Proof of Corollary 1

Particularizing to the LOS case $r_m = \sqrt{\beta}$, equation (18) implies that the two potential values of \tilde{g}_m are the same for all m . We denote these possible values by α and δ . Consider that M_s is the number of coefficients \tilde{g}_m set to δ and $M - M_s$ are set to α , with $M_s > 0$ (otherwise the zero distortion constraint cannot be satisfied). For a fixed value of M_s , applying the zero distortion constraint gives

$$\delta = -\alpha \left(\frac{M - M_s}{M_s} \right)^{1/3}.$$

Hence, setting M_s values of \tilde{g}_m to δ and $M - M_s$ to α give critical points of the Lagrangian. We fix $M/2 > M_s$ to avoid symmetrical/equivalent solutions. Among these critical points, we know from Appendix VII-B2c that only the critical points with $M_s = 1$ give maxima of the problem. In the LOS case, all of them are globally optimum as they achieve the same array gain. The SNR of the precoder $\text{SNR}_{\text{LOS}}^{\text{Z3RO}}$ in (12) is found by evaluating the array gain for the above values of the precoder at critical points. The SNR of the MRT can also be evaluated for the LOS channel giving

$$\text{SNR}^{\text{MRT}} = \frac{\beta p}{\sigma_v^2} M, \quad \text{SNR}_{\text{LOS}}^{\text{Z3RO}} = \frac{\beta p}{\sigma_v^2} M \frac{(\zeta^{2/3} - (1 - \zeta)^{2/3})^2}{\zeta^{1/3} + (1 - \zeta)^{1/3}},$$

where $\zeta = M_s/M$. For a fixed value of M_s , as $M \rightarrow \infty$, ζ goes to zero and the ratio of SNR goes to one. This concludes the proof of Corollary 1.

D. Proof of Proposition 2

We can define the gain at saturated antennas as

$$\begin{aligned} \gamma &= \left(\frac{\sum_{m'=M_s}^{M-1} r_{m'}^4}{\sum_{m''=0}^{M_s-1} r_{m''}^4} \right)^{1/3} \\ &= \left(\frac{M - M_s}{M_s} \right)^{1/3} \left(\frac{\frac{1}{M - M_s} \sum_{m'=M_s}^{M-1} r_{m'}^4}{\frac{1}{M_s} \sum_{m''=0}^{M_s-1} r_{m''}^4} \right)^{1/3}. \end{aligned}$$

The SNR of the heuristic precoder is given by

$$\begin{aligned} \text{SNR}^{\text{Z3RO}} &= \frac{p}{\sigma_v^2} \frac{(-\gamma \sum_{m \in \mathcal{M}} r_m^2 + \sum_{m' \notin \mathcal{M}} r_{m'}^2)^2}{\gamma^2 \sum_{m \in \mathcal{M}} r_m^2 + \sum_{m' \notin \mathcal{M}} r_{m'}^2} \\ &= \frac{p}{\sigma_v^2} M \frac{(-\gamma \frac{1}{M} \sum_{m \in \mathcal{M}} r_m + \frac{1}{M} \sum_{m' \notin \mathcal{M}} r_{m'})^2}{\gamma^2 \frac{1}{M} \sum_{m \in \mathcal{M}} r_m^2 + \frac{1}{M} \sum_{m' \notin \mathcal{M}} r_{m'}^2}. \end{aligned}$$

We can thus write the following ratio

$$\begin{aligned} \frac{\text{SNR}^{\text{Z3RO}}}{\text{SNR}_{\text{LOS}}^{\text{Z3RO}}} &= \frac{1}{\beta} \frac{(-\gamma \frac{1}{M} \sum_{m \in \mathcal{M}} r_m^2 + \frac{1}{M} \sum_{m' \notin \mathcal{M}} r_{m'}^2)^2}{\gamma^2 \frac{1}{M} \sum_{m \in \mathcal{M}} r_m^2 + \frac{1}{M} \sum_{m' \notin \mathcal{M}} r_{m'}^2} \\ &= \frac{\zeta^{1/3} + (1 - \zeta)^{1/3}}{(\zeta^{2/3} - (1 - \zeta)^{2/3})^2}. \end{aligned}$$

Given the i.i.d. property of the channel gain, as M and M_s grow large for a fixed value of the ratio M_s/M , γ converges to $\left(\frac{M - M_s}{M_s} \right)^{1/3}$. We can apply the same results to each average of i.i.d. terms appearing in the above expression. This gives

$$\begin{aligned} \frac{\text{SNR}^{\text{Z3RO}}}{\text{SNR}_{\text{LOS}}^{\text{Z3RO}}} &\rightarrow \frac{\left(-\left(\frac{M - M_s}{M_s} \right)^{1/3} \frac{M_s}{M} + \frac{M - M_s}{M} \right)^2}{\left(\frac{M - M_s}{M_s} \right)^{2/3} \frac{M_s}{M} + \frac{M - M_s}{M}} \\ &= \frac{\zeta^{1/3} + (1 - \zeta)^{1/3}}{(\zeta^{2/3} - (1 - \zeta)^{2/3})^2}. \end{aligned}$$

Using the change of variable $\zeta = M_s/M$ and rearranging terms, we find that the ratio goes to one. This concludes the proof.

REFERENCES

- [1] European Commission, "The European Green Deal," *COM (2019)*, p. 640, November 2019.
- [2] P. M. Lavrador, T. R. Cunha, P. M. Cabral, and J. Pedro, "The Linearity-Efficiency Compromise," *IEEE Microwave Magazine*, vol. 11, no. 5, pp. 44–58, 2010.
- [3] S. Muneer, L. Liu, O. Edfors, H. Sjöland, and L. Van der Perre, "Handling PA Nonlinearity in Massive MIMO: What are the Tradeoffs Between System Capacity and Power Consumption," in *2020 54th Asilomar Conference on Signals, Systems, and Computers*, 2020, pp. 974–978.
- [4] C. Fager, T. Eriksson, F. Barradas, K. Hausmair, T. Cunha, and J. C. Pedro, "Linearity and Efficiency in 5G Transmitters: New Techniques for Analyzing Efficiency, Linearity, and Linearization in a 5G Active Antenna Transmitter Context," *IEEE Microwave Magazine*, vol. 20, no. 5, pp. 35–49, 2019.

- [5] N. N. Moghadam, G. Fodor, M. Bengtsson, and D. J. Love, "On the Energy Efficiency of MIMO Hybrid Beamforming for Millimeter-Wave Systems With Nonlinear Power Amplifiers," *IEEE Transactions on Wireless Communications*, vol. 17, no. 11, pp. 7208–7221, 2018.
- [6] S. Teodoro, A. Silva, R. Dinis, F. M. Barradas, P. M. Cabral, and A. Gameiro, "Theoretical Analysis of Nonlinear Amplification Effects in Massive MIMO Systems," *IEEE Access*, vol. 7, pp. 172 277–172 289, 2019.
- [7] E. G. Larsson and L. Van der Perre, "Out-of-Band Radiation From Antenna Arrays Clarified," *IEEE Wireless Communications Lett.*, vol. 7, no. 4, pp. 610–613, 2018.
- [8] C. Mollén, U. Gustavsson, T. Eriksson, and E. G. Larsson, "Spatial Characteristics of Distortion Radiated From Antenna Arrays With Transceiver Nonlinearities," *IEEE Trans. on Wireless Commun.*, vol. 17, no. 10, pp. 6663–6679, 2018.
- [9] Y. Zou, O. Raeesi, L. Antilla, A. Hakkarainen, J. Vieira, F. Tufvesson, Q. Cui, and M. Valkama, "Impact of Power Amplifier Nonlinearities in Multi-User Massive MIMO Downlink," in *2015 IEEE Globecom Workshops (GC Wkshps)*, 2015, pp. 1–7.
- [10] F. Rottenberg, G. Callebaut, and L. Van der Perre, "Spatial Distribution of Distortion due to Nonlinear Power Amplification in Distributed Massive MIMO," in *2021 IEEE 22nd International Workshop on Signal Processing Advances in Wireless Communications (SPAWC)*, 2021, pp. 76–80.
- [11] C. Hemmi, "Pattern characteristics of harmonic and intermodulation products in broadband active transmit arrays," *IEEE Trans. on Antennas and Propagation*, vol. 50, no. 6, pp. 858–865, 2002.
- [12] S. K. Mohammed and E. G. Larsson, "Per-Antenna Constant Envelope Precoding for Large Multi-User MIMO Systems," *IEEE Trans. on Commun.*, vol. 61, no. 3, pp. 1059–1071, 2013.
- [13] B. Krongold and D. Jones, "An active-set approach for OFDM PAR reduction via tone reservation," *IEEE Transactions on Signal Processing*, vol. 52, no. 2, pp. 495–509, 2004.
- [14] S. C. Cripps, *RF Power Amplifiers for Wireless Communications*. Artech house Norwood, MA, 2006, vol. 2.
- [15] N. Tervo, B. Khan, O. Kursu, J. P. Aikio, M. Jokinen, M. E. Leinonen, M. Juntti, T. Rahkonen, and A. Pärssinen, "Digital Predistortion of Phased-Array Transmitter With Shared Feedback and Far-Field Calibration," *IEEE Trans. on Microwave Theory and Techniques*, vol. 69, no. 1, pp. 1000–1015, 2021.
- [16] C. Tarver, A. Balatsoukas-Stimming, C. Studer, and J. R. Cavallaro, "OFDM-Based Beam-Oriented Digital Predistortion for Massive MIMO," in *2021 IEEE International Symposium on Circuits and Systems (ISCAS)*, 2021, pp. 1–5.
- [17] C. Tarver, A. Balatsoukas-Stimming, C. Studer, and J. R. Cavallaro, "Virtual DPD Neural Network Predistortion for OFDM-based MU-Massive MIMO," in *2021 55th Asilomar Conference on Signals, Systems, and Computers*, 2021, pp. 376–380.
- [18] L. Antilla, A. Brihuega, and M. Valkama, "On Antenna Array Out-of-Band Emissions," *IEEE Wireless Communications Letters*, vol. 8, no. 6, pp. 1653–1656, 2019.
- [19] S. R. Aghdam, S. Jacobsson, U. Gustavsson, G. Durisi, C. Studer, and T. Eriksson, "Distortion-Aware Linear Precoding for Massive MIMO Downlink Systems with Nonlinear Power Amplifiers," *arXiv preprint arXiv:2012.13337*, 2020.
- [20] N. Kolomvakis, M. Bavand, I. Bahceci, and U. Gustavsson, "A Distortion Nullforming Precoder in Massive MIMO Systems with Nonlinear Hardware," *IEEE Wireless Communication Letters*, 05 2022.
- [21] R. Zayani, H. Shaïek, and D. Roviras, "Efficient Precoding for Massive MIMO Downlink Under PA Nonlinearities," *IEEE Communications Letters*, vol. 23, no. 9, pp. 1611–1615, 2019.
- [22] I. Iofedov and D. Wulich, "Distortion cancellation precoding for OFDM-SDMA downlink with nonlinear power amplifiers," in *2015 IEEE 26th Annual International Symposium on Personal, Indoor, and Mobile Radio Communications (PIMRC)*, 2015, pp. 704–709.
- [23] F. Rottenberg, G. Callebaut, and L. Van der Perre, "Z3RO Precoder Canceling Nonlinear Power Amplifier Distortion in Large Array Systems," in *ICC 2022 - IEEE International Conference on Communications*, 2022, (accepted).
- [24] T. Feys, G. Callebaut, L. Van der Perre, and F. Rottenberg, "Measurement-Based Validation of Z3RO Precoder to Prevent Nonlinear Amplifier Distortion in Massive MIMO Systems," in *(accepted) 2022 IEEE 93rd Vehicular Technology Conference (VTC2022-Spring)*, 2022.
- [25] A. Paulraj, A. P. Rohit, R. Nabar, and D. Gore, *Introduction to space-time wireless communications*. Cambridge university press, 2003.
- [26] J. Tellado, L. Hoo, and J. Cioffi, "Maximum-likelihood detection of nonlinearly distorted multicarrier symbols by iterative decoding," *IEEE Transactions on Communications*, vol. 51, no. 2, pp. 218–228, 2003.
- [27] C. Rapp, "Effects of HPA-Nonlinearity on a 4-DPSK/OFDM-Signal for a Digital Sound Broadcasting System," in *Proceedings of the Second European Conference on Satellite Communications, ECSC-2, Liège, Belgium*, 1991.
- [28] J. J. Bussgang, "Crosscorrelation functions of amplitude-distorted Gaussian signals," 1952.
- [29] Ö. T. Demir and E. Björnson, "The bussgang decomposition of nonlinear systems: Basic theory and MIMO extensions," *arXiv preprint arXiv:2005.01597*, 2020.